Benchmarking ionizing space environment models

Sebastien Bourdarie, Christophe Inguimbert, Denis Standarovski, Jean-Roch Vaillé, Angelica Sicard-Piet, Didier Falguere, Robert Ecoffet, Christian Poivey, Eric Lorfèvre

Benchmarking ionizing space environment models

S. Bourdarie, C. Inguimbert, D. Standarovski, J.-R. Vaillé, A. Sicard-Piet, D. Falguere, R. Ecoffet, C. Poivey, E. Lorfèvre

***Abstract:* In flight feedback data are collected such as displacement damage doses, ionizing doses and cumulated SEUs on board various space vehicles and are compared to predictions performed with (1) proton measurements performed with spectrometers data on board the same spacecraft if any and (2) protons spectrum predicted by the legacy AP8min model and the AP9 and OPAL models. When an accurate representation of the 3D spacecraft shielding as well as appropriate ground calibrations are considered in the calculations such comparisons provide powerful metrics to investigate engineering model accuracy. To describe > 30 MeV trapped protons fluxes, AP8 min model is found to provide closer predictions to observations than AP9 V1.30.001 (Mean and Perturbed mean).**

I. Introduction

Because of their harmful effects on human bodies and spacecraft electronics, the Earth's radiation belts have been intensively studied since their discovery in 1958. Spacecraft engineers need a reliable and statistical description of the belts to design space missions. The current standard models, AE8 [1] and AP8 [2], were developed by NASA at the end of the 1970s and beginning of the 1980s. Different studies have put forward their shortcomings ([3] and [4]): inadequate resolution at low altitude, no variability on time-scales less than a solar cycle, etc. To overcome these limitations a recent effort in the US has allowed to release the AE9 and AP9 specification models [4].

To better validate and control uncertainties on space environment specification models, a new tool has been developed in order to perform quick and accurate Benchmark of Ionizing Space Environment models (BISE). The main goal is to collect in flight measurements which are independent of specification models construction in order to ensure a fully independent validation. Accordingly, total ionizing dose (TID), displacement damage dose (DDD) measurements and cumulative SEU EDAC counters are favored. Then, to evaluate the measured degradation, it is of prime importance to collect details of the spacecraft, payload, electronic board and chip shielding, the ground calibrations of dosimeters, and diodes, or the cross-section of interaction to trigger a SEE in a memory.

In Section II, the BISE tool allowing to fly any spacecraft into existing space environment specification model and to deduce measured effects is described. In Section III flight data are presented and compared to model predictions and in Section IV uncertainties in models such as AP8 and AP9 are discussed.

II. BISE tool

The Benchmark of Ionizing Space Environment models tool (BISE) is written in IDL (Interactive Data Language) and is set to provide all functionalities to build up a data base of in flight effect measurements, to plot support data, (i.e. shielding description around the parts under study, response function of the parts to the environment ..), to compute the effects (TID, DDD, cumulated SEU, …) predicted from specification models and to plot a comparison between model predictions and in flight observations (Fig. 1).

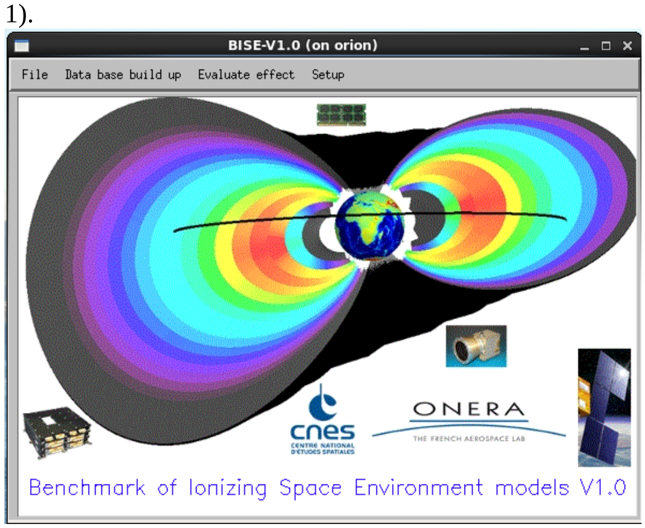

Fig. 1: Main window of the BISE tool (after [8])

First of all, it is necessary to propagate the orbit of the spacecraft of interest (along which an effect under study could be further undertaken). To do so, the TLE (Two-Line Element) orbit determination sets are retrieved from NORAD [5] and the spacecraft orbit is propagated with a 20 seconds time step for the mission duration based on the Simplified General Perturbation 4 [6] software (SGP4) using the BISE tool.

Secondly, trapped electron and proton specification environment models are implemented in the BISE software so that it is convenient to fly any spacecraft in the model of interest. So far, AE8/AP8 min and max [1], AE9/AP9 V1.20.002 and V1.30.001 Mean, Perturbed and Monte-Carlo

---

This work was supported by grant n° R-S12/MT-0003-107 which is part of CNES R&T program.

S. Bourdarie, C. Inguimbert, A. Sicard-Piet, D. Falguere are with ONERA The French aerospace lab/Département Environnement Spatial, 31400 Toulouse France (telephone; +33-562-2756, fax : +33-562-2569, e-mail: Sebastien.Bourdarie@onera.fr).
J.R. Vaillé is with the Université Montpellier 2-IES, 34095 Montpellier cedex 5, France, and also with the Université de Nimes, 30021 Nimes, France
E. Lorfèvre, R. Ecoffet and D. Standarovski are with CNES, 18 av. E. Belin 31401 Toulouse, France
C. Poivey is with ESA-ESTEC, Keplerlaan 1 P.O. Box 299, 2200 AG Noordwijk ZH, The Netherlands

[4] and the Onera Proton Altitude Low, OPAL, [7] are implemented in the tool. The OPAL specification model can be run for any orbit with altitudes below than 800 km and provides trapped proton fluxes for energies between 40 MeV and 650 MeV. The interface allows to select a spacecraft registered in the database, a time period, a specification environment model with corresponding available versions and options and then retrieving the trapped environment along the orbit with a 20 seconds time step. Note that when a new specification model version comes up (as it is quite often the case with AE9/AP9) it is straightforward to include it in the tool. The trapped particle fluences from beginning of mission to each time when an effect measurement is available can be evaluated to predict any cumulative effect (TID, DDD, and cumulated SEU).

The BISE tool allows plotting support data as well, like the details being available to describe the 3D shielding around the electronic chip under study from a FASTRAD sectoring analysis (the output ascii file from FASTRAD must be provided to the BISE tool which can plot the 3D shielding as a fish eye view, back and front side or shielding thickness distribution) [9]. Three typical details of 3D spacecraft description are found, “no spacecraft”, “6 faces” or “full” and can be consider evaluating an effect. The response function of the chip to the environment can also be plotted, like the damage factor versus incident energy or ionizing dose factor versus incident energy (the response function must be computed outside of the BISE tool and must be provided as a two column ascii file) … Impact of different description of the 3D shielding can be analyzed and compared in an easy way.

Finally the tool evaluates cumulative effects measurements available in the database for all environment models that have been computed along the orbit of interest (see [23] for more details):

$$Effect\,(T) = \int_{0}^{T} \int_{E=1MeV}^{E=2GeV} \frac{d\Phi}{dE}(E,t) \cdot RF(E) \cdot dE \cdot dt \quad (1)$$

where RF(E) is the response function, $\frac{d\Phi}{dE}$ the omnidirectional flux, and E the incident particle energy. Note that the integral over the energy is limited to 1 MeV to 2 GeV because (1) the response function of the effects being investigated here is always 0 for protons with energy below 1 MeV (they are stopped in the shielding) and (2) the trapped proton fluxes are always 0 for energies above 2 GeV (maximum proton energy in AP8 is 300 MeV and maximum proton energy in AP9 is 2 GeV).

III. In flight data and comparison to model predictions

We concentrate here, on proton specification model validation. The in-flight data available in the current study are organized according to increasing altitude.

A. Total Displacement Damage Dose (DDD) at 660 km altitude

SAC-D is an Argentinean spacecraft from CONAE flying on a Low Earth Orbit (circular orbit: 660 km, inclination: 98°, 14.12 revolutions/day). It was launched on June 10, 2011. One of the payloads is the ICARE-NG [10] instrument which was built in the frame of the CARMEN-1 (“CARactérisation et Modélisation de l’ENvironnement”) suite (composed of ICARE-NG and SODAD instruments which have been funded by CNES). The ICARE-NG instrument on-board SAC-D began its operation in August 30, 2011 and stopped in June 7th 2015.

DDD is evaluated using the degradation of a Light Emitting Diode (LED) embedded in an OSL (Optically Stimulated Luminescence) sensor which is part of the ICARE-NG instrument. The LED was fully calibrated before launch, in terms of sensitivity to temperature and current through the LED versus DDD. All details about the instrument and data analysis can be found in [11]-[15]. The time resolution for the DDD is 6 hours and data from August 30, 2011 to June 7th, 2015 are considered. Careful attention was taken to correct the temperature effect on the current through the LED (the temperature of the ICARE-NG is part of the housekeeping data of the instrument, see [15] for more details). Also, the conversion from LED current to DDD is done according to ground calibration [16].

To calculate an accurate DDD of the LED part of the OSL sensor, the 3D shielding around the OSL must be well known. The distribution of shielding thicknesses seen by the OSL sensor on board SAC-D was calculated by a sector analysis carried out by the TRAD company using the FASTRAD software [9] (Fig. 2). The solid angle viewed from the LED is decomposed into 80000 sectors of equal value (200 steps in polar angles and 400 steps in azimuthal angles). The shielding around the OSL sensor can be represented like two "fish eye" views **(**Fig. 3), one forward (2π steradians) and the other backward (2π other steradians).

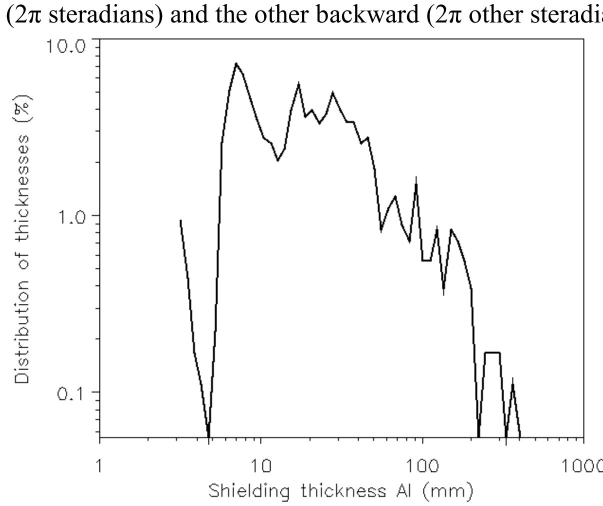

Fig. 2: Distribution of Al equivalent shielding thicknesses (in mm) as viewed by the OSL sensor on board SAC-D spacecraft (after [8]).

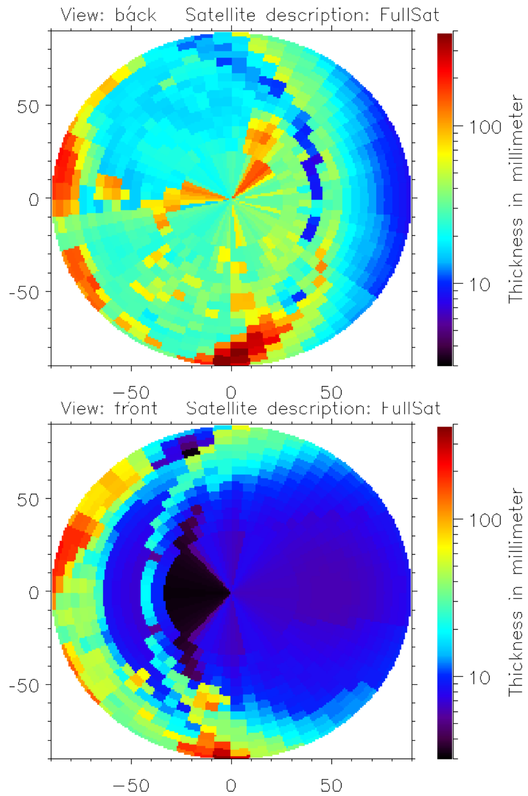

Fig. 3: "Fish eye" views of the shielding around the OSL sensor on-board SAC-D spacecraft; bottom is forward (2π steradians) and top is backward (2π other steradians). Color scale is in mm.

Then, the response function RF(E) of the OSL sensor (Fig. 4) is calculated according to [23] as a function of proton incident energy, E (MeV), assuming $\frac{d\Phi}{dE}=1$ (MeV^{-1} cm^{-2} s^{-1}).

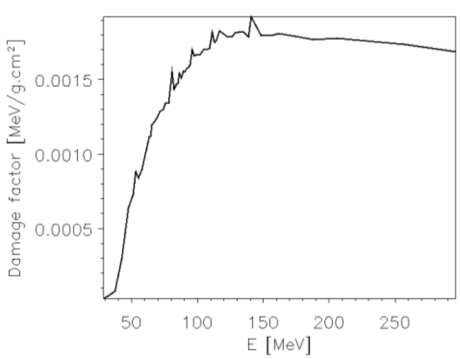

Fig. 4: Response function of damage factor of the OSL sensor on board SAC-D spacecraft considering isotropic proton incidence versus proton energy (after [8]).

The ICARE-NG instrument is also composed of a radiation monitor. Two telescopes (A and C) and a single detector (B) allow for measurements of electrons and protons fluxes in the energy range 250 keV-3.2 MeV and 12.8-190 MeV, respectively [17]. The time resolution is 16s. The integral channels, being omnidirectional, are used to retrieve the trapped proton environment at SAC-D altitude along the mission.

A comparison of the mission average trapped proton spectrum deduced from AP8 min, AP9 Mean V1.30.001, AP9 Perturbed Mean V1.30.001 median out of 40 scenarios, OPAL and ICARE_NG models and data is given in Fig. 5. For energy greater than 40 MeV (proton energies reaching the OSL sensor) AP9 V1.30.001 (Mean or Perturbed Mean) fluxes are the highest ones while AP8 min fluxes are the lowest ones, the differences being less than a factor 2. Note that AP9 Mean V1.30.001 and V1.20.002 provide exactly the same results at SAC-D altitude.

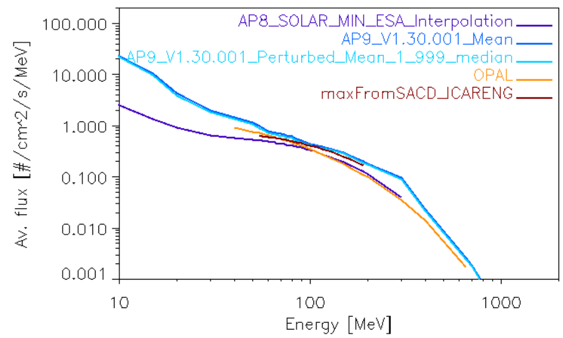

Fig. 5: Comparison of the mission average trapped proton spectrum at SAC-D orbit deduced from AP8 min, AP9 Mean V1.30.001, AP9 Perturbed Mean V1.30.001 median out of 40 scenarios, OPAL and ICARE_NG models and data.

A comparison of cumulated OSL sensor DDD predicted from ICARE-NG spectrometers, AP8 min, AP9 Mean V1.30.001 and AP9 Perturbed Mean V1.30.001 median out of 40 scenarios is shown in Fig. 6. The spectra from each mode were imputed into Eq. 1 using the same shielding and response function. It turns out that the OSL DDD measures and those predicted from the ICARE-NG spectrometer measurements are within 12%. AP8 min [1] and OPAL [7] specification models underestimate the OSL DDD by respectively, 11.3% and 9.3% while AP9 Mean V1.30.001 and AP9 Perturbed Mean V1.30.001 median out of 40 scenarios [4] overestimates the OSL DDD by respectively 41.6% and 32.6%.

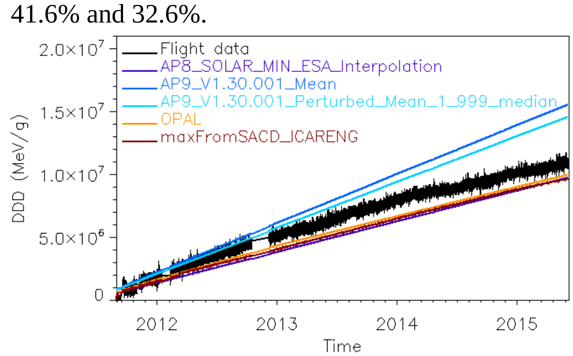

Fig. 6: Comparison of the measurements of the OSL DDD on board SAC-D spacecraft with those derived from the proton measurement with the ICARE-NG spectrometers, AP8 min, AP9 Mean V1.30.001, AP9 Perturbed Mean V1.30.001 median out of 40 scenarios and OPAL along a 660 km altitude, 98° inclination orbit (after [8]).

B. SEU from EDAC counter at 719 km altitude

CRYOSAT-2 is a European Space Agency satellite flying on a Low Earth Orbit (near circular orbit: 719-730 km, inclination: 92°, 14.52 revolutions/day). It was launched on

April 8th 2010. One of the payloads is the SAR Interferometer Radar Altimeter (SIRAL) being built by Thales Alenia Space (TAS). This altimeter, whose memory map is made of 10 SRAM (1MB SRAM M65608, 0.5µm CMOS process, developed by ATMEL in cooperation with the European Space Agency), is continuously exposed to space radiation environment, inducing Single Event Phenomena (bit flips) on the memory points of the mass storage. These errors are automatically corrected, listed by the EDAC counter and downloaded on ground station every month.

The SEU recorded by the EDAC from November 1st, 2010 to December 31st, 2015 are plotted in a longitude-latitude map in Fig. 7. The two black curves indicates the magnetic field lines L=1.9 at CRYOSAT-2 altitude. To sort out SEUs induced by trapped protons in the radiation belts to those induced by GCRs or Solar energetic particles (SEP), the SEUs recorded at locations below L=1.9 (in between the two black curves of Fig. 7) are attributed to trapped protons. Clearly, most SEUs are recorded in the South Atlantic Anomaly (88.4%). The SEUs at high and low latitudes can be attributed to GCRs and SEPs (11.6%).

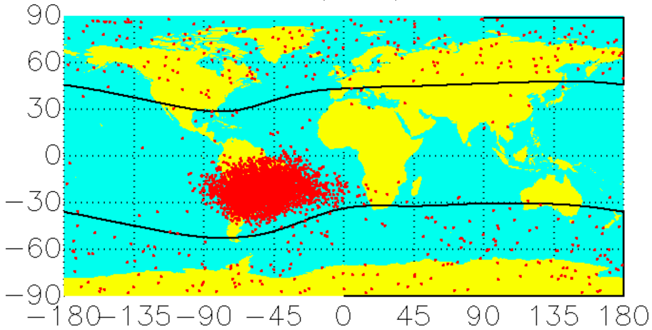

Fig. 7: SEU recorded by the EDAC implemented on the CRYOSAT-2/SIRAL payload from November 1st, 2010 to December 31st, 2015.

To calculate an accurate SEU rate of mass memory of the SIRAL payload, the 3D shielding around the SRAM device must be well known. The distribution of shielding thicknesses seen by the SRAM device on board CRYOSAT-2/SIRAL was calculated by a sector analysis carried out by TAS company using the FASTRAD software [9] (Fig. 8). The solid angle viewed from the SRAM M65608 is decomposed into 1800 sectors of equal value (30 steps in polar angles and 60 steps in azimuthal angles). The corresponding two "fish eye" views are presented in Fig. 9.

The M65608 SRAM has been tested under heavy ions and proton beams by ESA. In particular, three test campaigns under proton beam were performed, they are denoted “ESA 1997” [18], “RADECS 2005” [19] and “TRAD 2013” [20]. The SEU cross section versus proton energy is given in Fig. 10 and can be fitted by a Weibull fit function with the following parameters: W=18, s=1.5. An energy threshold of 15 MeV and a saturated cross section of 5.28 10^{-8} cm^2/device can be found. Note that the three test campaigns allow to determine the saturated cross section with a very good accuracy. This is a key point for the following analysis.

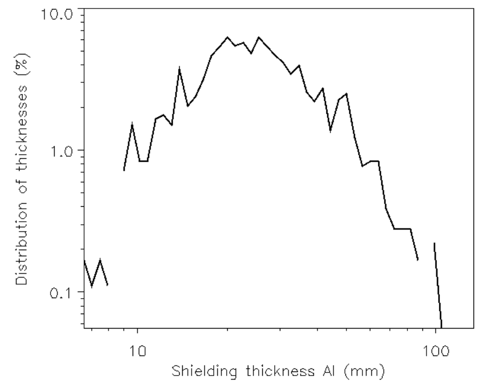

Fig. 8: Distribution of Al equivalent shielding thicknesses (in mm) as viewed by the SRAM device on board CRYOSAT-2/SIRAL spacecraft.

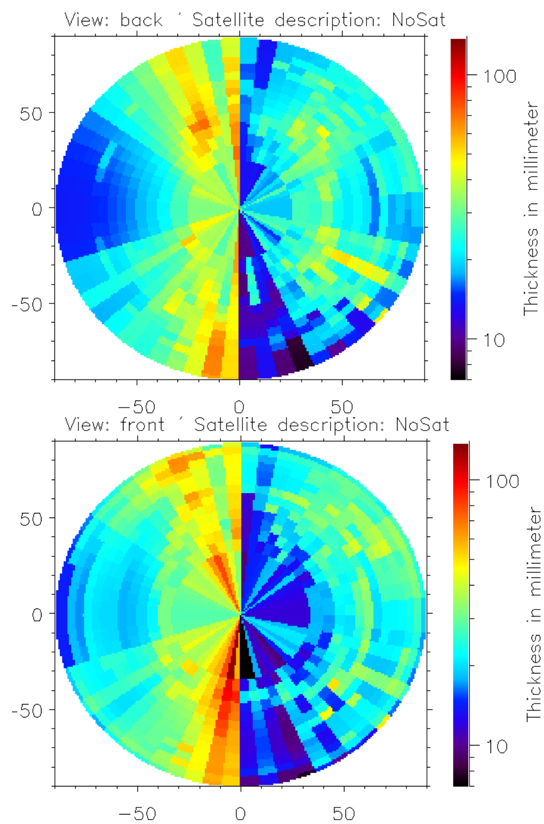

Fig. 9: "Fish eye" views of the shielding around the SRAM device on-board CRYOSAT-2 spacecraft; bottom is forward (2π steradians) and top is backward (2π other steradians). Color scale is in mm.

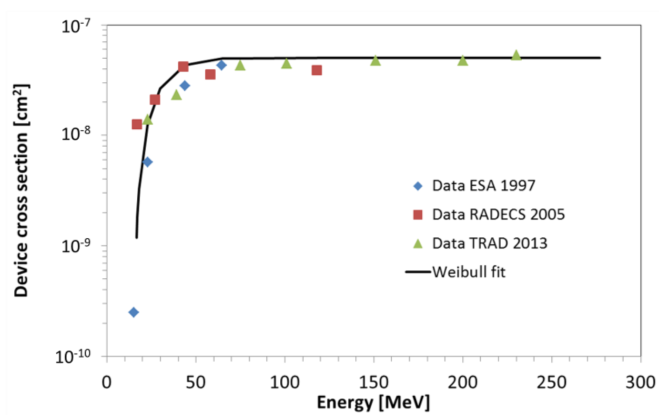

Fig. 10: M65608 SRAM device cross section versus proton energy.

A comparison of the mission average trapped proton spectrum deduced from AP8 min, AP9 Mean V1.30.001, AP9 Perturbed Mean V1.30.001 median out of 40 scenarios and OPAL models is given in Fig. 10. For energy greater than 40 MeV (proton energies reaching the chip) AP9 V1.30.001 (Mean or AP9 Perturbed Mean median out of 40 scenarios) fluxes are the highest ones while AP8 min fluxes are the lowest ones, the differences being less than a factor 2. Like at SAC-D altitude, AP9 Mean V1.30.001 and V1.20.002 provide exactly the same results at CRYOSAT-2 altitude.

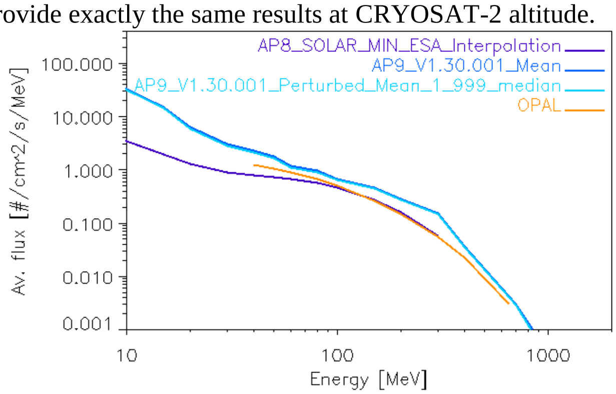

Fig. 11: Comparison of the mission average trapped proton spectrum at CRYOSAT-2 orbit deduced from AP8 min, AP9 Mean V1.30.001, AP9 Perturbed Mean V1.30.001 median out of 40 scenario and OPAL models.

The transmitted proton flux at the chip level is calculated (external to the BISE tool calculation) from a MCNPx [21][22] (Monte-Carlo N-Particle eXtended) V2.7.0 Monte-Carlo run accounting for the 3D shielding surrounding the chip (Fig. 12). In the transmitted AP8 min flux, a cutoff at 300 MeV is found while AP9 V1.30.001 or OPAL transmitted spectra extend to higher energy. This is resulting from the upper energy limit being described by the models. The efficiency of proton transport through the 3D shielding is given in Fig. 13. Note that incident protons with energy less than 48 MeV will be fully stopped by the shielding surrounding the chip.

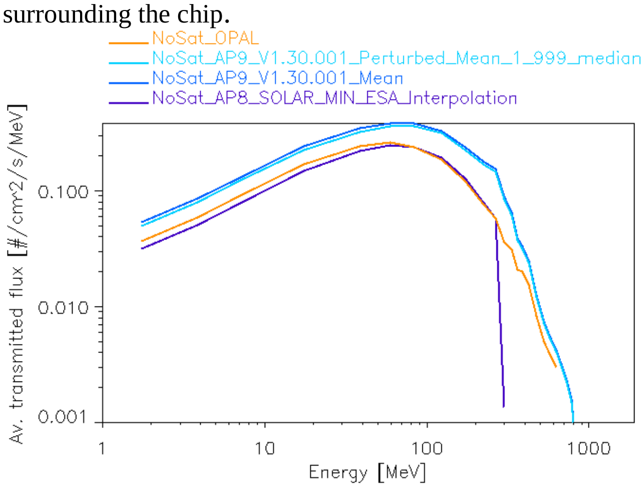

Fig. 12: Transmitted differential proton flux at the CRYOSAT-2/SIRAL/ chip level deduced from AP8 min, AP9 Mean V1.30.001, AP9 Perturbed Mean V1.30.001 median out of 40 scenarios and OPAL models.

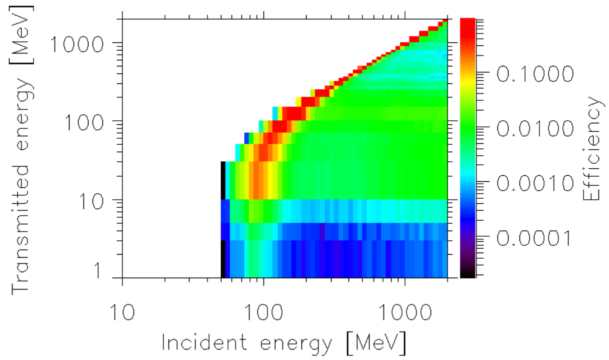

Fig. 13: Proton transport efficiency through the 3D shielding surrounding the chip on SIRAL payload.

A comparison of cumulated SEUs predicted from AP8 min and AP9 V1.30.001 (Mean and Perturbed Mean – median out of 40 scenarios) is shown in Fig. 14. It turns out that the cumulated SEUs flight data and those predicted from OPAL model are very much comparable. A difference of 0.6% is found. Note that a solar cycle inflection is found in the flight data but is rather weak. As OPAL [7] model is solar cycle dependent, an inflection is also found from OPAL cumulated SEUs predictions. AP8 min [1] specification model underestimates the cumulated SEUs by 12.3% while AP9 V1.30.001 Mean and Perturbed mean [4] overestimate the cumulated SEUs by respectively 82% and 72.7%. While AP8 min and OPAL transmitted fluxes with energy from 15 to 300 MeV are very much similar, the predicted cumulated SEUs are somewhat different. This is caused by the AP8 min cutoff at 300 MeV. The tail of the transmitted flux is important to calculate very accurate cumulated SEUs (unless the device cross section is very well defined).

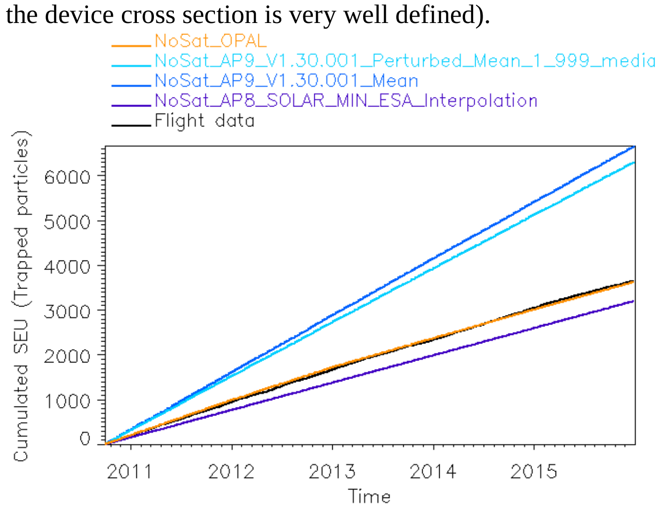

Fig. 14: Comparison of the cumulated SEUs measured by the EDAC on board CRYOSAT-2/SIRAL and predicted from AP8 min, AP9 Mean V1.30.001, AP9 Perturbed Mean V1.30.001 median out of 40 scenarios and OPAL models.

C. *Total Displacement Damage Dose (DDD) at 1336 km altitude*

In [23] in-flight displacement damage on the OSL sensor was compared with prediction performed with space environment measured on board JASON-2 spacecraft as well as with prediction performed with AP8min and AP9V1.05 specification models.

In the current study an update is provided, where more recent in-flight data have been added and AP9 V1.30.001 has been used (Fig. 15). Note that the energy integration in Eq. 1 has been improved since [23] such as an integration using a five-point Newton-Cotes integration formula was preferred to the integration by the method of the trapezoids.

The updated results are very consistent with conclusions in [23]:

- AP8min underestimates the DDD by 16.2%
- AP9 V1.30.001 Mean and Perturbed mean-median out of 40 scenarios overestimates DDD by respectively 113% and 110%.
- Predictions from ICARE-NG spectrometers are within 4.8% to DDD flight data.

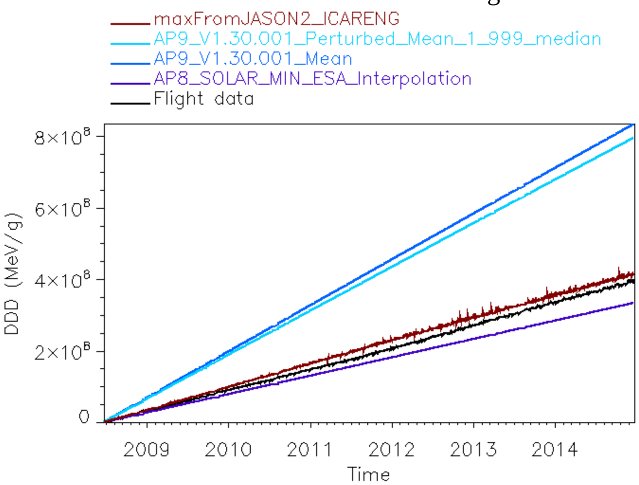

Fig. 15: Comparison of the measurements of the OSL DDD on board JASON-2 spacecraft with those derived from the proton measurement with the ICARE-NG spectrometers and AP8 min, AP9 Mean V1.30.001and AP9 Perturbed Mean V1.30.001 median out of 40 scenarios along a 1336 km altitude, 63° inclination orbit (after [8]).

D. SEU from EDAC counter at 1336 km altitude

One of the payloads onboard JASON-2 spacecraft is the same SAR Interferometer Radar Altimeter (SIRAL) being built by Thales Alenia Space (TAS) as the one flying on CRYOSAT-2. The SEUs affecting the 10 SRAM (1MB SRAM M65608, 0.5µm CMOS process, developed by ATMEL in cooperation with the European Space Agency) are automatically corrected, listed by the EDAC counter and downloaded on ground station on a regular basis.

The SEU recorded by the EDAC from June 22nd, 2008 to December 31st, 2011 are plotted in a longitude-latitude map in (Fig. 16). The two black curves indicates the magnetic field lines L=1.9 at JASON-2 altitude. As for CRYOSAT-2 events, to sort out SEUs induced by trapped protons to those induced by GCRs and SPEs, the SEUs recorded at locations below L=1.9 (in between the two black curves of Fig. 16) are attributed to trapped protons. Again, most SEUs are recorded in the South Atlantic Anomaly (98.8%) and can be attributed to trapped protons in the radiation belts. The SEUs at high and low latitudes can be attributed to GCRs and SEPs (1.2%).

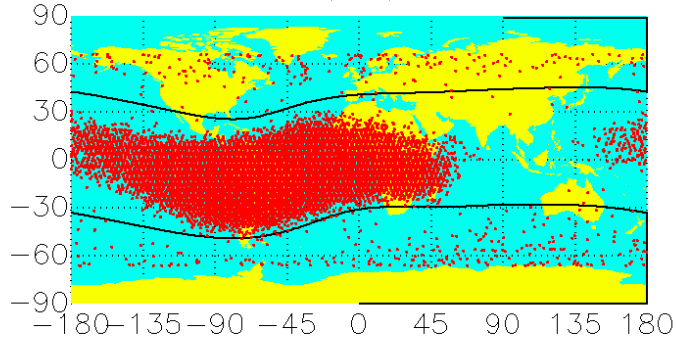

Fig. 16: SEU recorded by the EDAC implemented on the JASON-2/SIRAL payload from June 22nd, 2008 to December 31st, 2011.

A comparison of the mission average trapped proton spectrum deduced from AP8 min and AP9 Mean V1.05 Models, and ICARE_NG data was given in [23]. Note that at JASON-2 altitude AP9 Mean V1.05 is equal to V1.30.001. The transmitted proton flux at the chip level is computed using the same efficiency matrix as for CRYOSAT-2/SIRAL and is shown in Fig. 17. As was found in [23], AP9 V1.30.001 (Mean and Perturbed mean- median out of 40 scenarios) trapped proton flux prediction is well above those from AP8 or ICARENG data. In the transmitted AP8 min flux and ICARE_NG, a cutoff at 300 MeV is found while AP9 V1.30.001 Mean and Perturbed mean transmitted spectra extend to higher energy. This is resulting from the upper energy limit being described by AP8 min model and the highest proton channel available on-board JASON-2/ICARE_NG (being 292 MeV).

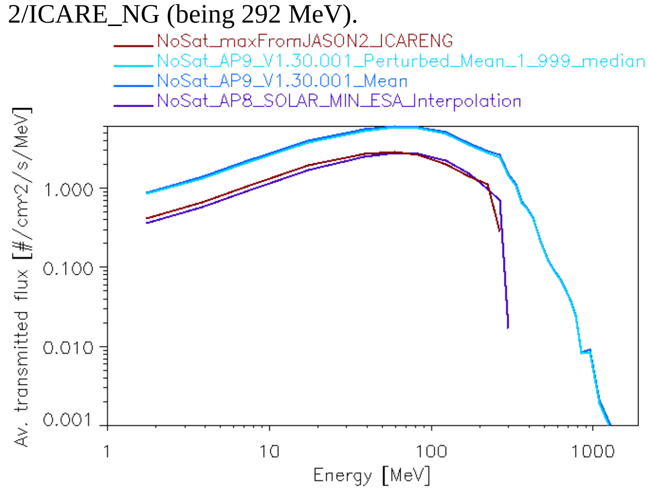

Fig. 17: Transmitted differential proton flux at the JASON-2/SIRAL/ chip level deduced from AP8 min and AP9 Mean V1.30.001, AP9 Perturbed Mean V1.30.001 median out of 40 scenarios models and JASON-2/ICARENG data.

A comparison of cumulated SEUs predicted from AP8 min and AP9 V1.30.001 Mean and Perturbed mean-median out of 40 scenarios models and ICARE_NG data is shown in Fig. 20. AP8 min [1] specification model and ICARE_NG data underestimates the cumulated SEUs by 28.5% and 31.5% respectively while AP9 Mean V1.30.001 and AP9 Perturbed Mean V1.30.001 median out of 40 scenarios [4] overestimates the cumulated SEUs by respectively 104% and 95.1%. As mentioned for CRYOSAT-

2/SIRAL/EDAC prediction, this prediction made using AP8 min or ICARE_NG data are affected by the energy cutoff at 300 MeV. The tail of the transmitted flux is important to calculate very accurate cumulated SEUs (unless the device cross section is very well defined). Note that the deviation found here from AP9 Mean 1.30.001 is fully consistent with the deviation found when comparing with DDD prediction of the OSL onboard JASON-2/ICARE_NG/OSL.

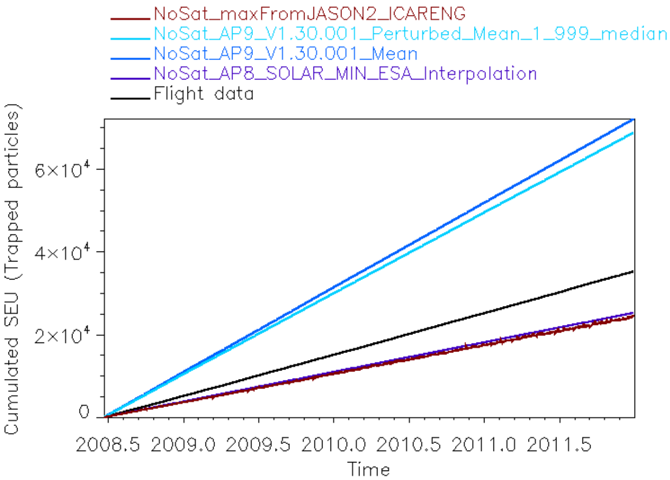

Fig. 18: Comparison of the cumulated SEUs measured by the EDAC on board JASON-2/SIRAL and predicted from AP8 min, AP9 V1.30.001 Mean and Perturbed mean-median out of 40 scenarios and OPAL models.

E. Total Ionising Dose (TID) at 8070 km altitude

O3B is a satellite constellation built by Thales Alenia Space and operated by O3B Networks Ltd. The orbit is circular at 8070 km altitude, 0° inclination. The first four satellites were launched on 25 June 2013, and eight more in 2014. Inside the payload interface unit (PLIU) of each spacecraft, a RadFET manufactured by Tyndall National Institute and provided by ESA is implemented [24]. The RadFET gate oxide thickness is 400 nm.

Two calibration campaigns were conducted, one at ESA and one at TRAD facility using Co^{60} radiation source, respecting the exact implementation of the RadFET into the O3B/PLIU. So far irradiation runs were performed at room temperature, i.e. 25°C, to provide threshold voltage shift of the RadFET versus dose levels received.

To calculate an accurate TID of the RadFET, the 3D shielding around the chip must be well known. The distribution of shielding thicknesses seen by the RadFET on board O3B was calculated by a sector analysis carried out by Thales Alenia Space using the FASTRAD software [7] (Fig. 19). Then, the response function RF(E) of the RadFET (Fig. 20) is calculated from a MCNPx V2.7.0 Monte-Carlo run .

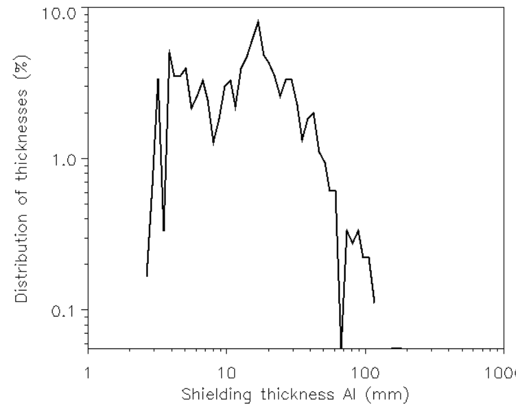

Fig. 19: Distribution of Al equivalent shielding thicknesses (in mm) as viewed by the RadFET on board O3B spacecraft (after [8]).

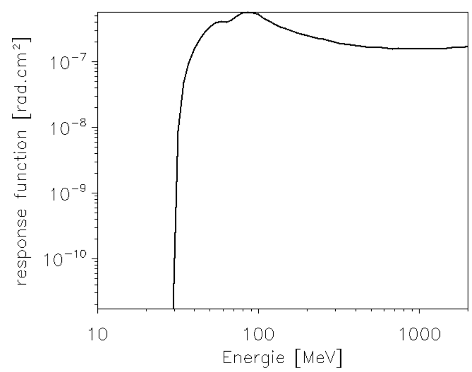

Fig. 20: Response function of ionizing dose factor of the RadFET implemented in the O3B/PLIU considering isotropic proton incidence versus proton energy (after [8]).

A comparison of TID predicted from AP8 min and AP9 V1.30.001 Mean and Perturbed mean-median out of 40 scenarios is shown in Fig. 21. The spectra from each model were imputed into Eq. 1 using the same response function shown in Fig. 22. The results indicate that AP8 min, AP9 Mean V1.30.001 and AP9 V1.30.001 Perturbed mean-median out of 40 scenarios overestimates the TID by 161%, 1235% and 1234% respectively.

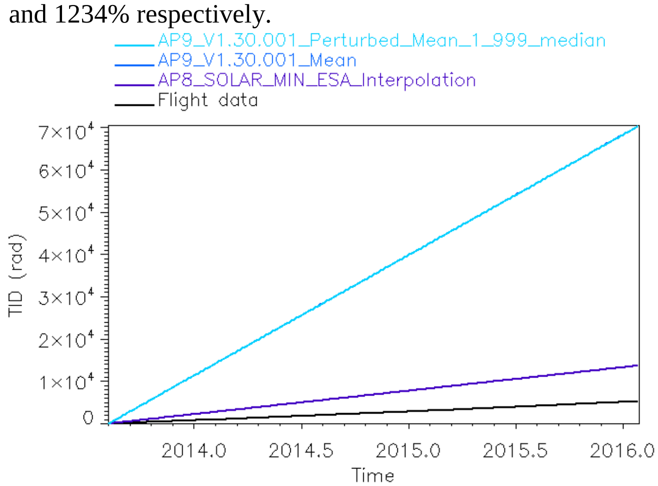

Fig. 21: Comparison of the measurements of the TID with those derived from AP8 min AP9 Mean V1.30.001 and AP9 Perturbed Mean V1.30.001 median out of 40 scenarios along a 8070 km altitude, 0° inclination orbit (after [8]). The two AP9 curves are overplotted.

V CONCLUSIONS

In-flight data showing cumulated effects such as DDD, TID and SEUs from EDAC counters have been used to investigate uncertainties in trapped proton specification models. Because careful attention was paid to incorporate the full 3D spacecraft geometry in the calculations as well as appropriate ground calibrations of the OSL/LED, the ESA-RaDFET and the M65608 SRAM all errors in the process are under control.

In the 660 to 720 km altitude range, deviations found between in-flight measurements and predictions from specification models are very consistent whether validation is done against displacement damage or cumulated SEUs from EDAC counter. This global coherence indicates that results are unlikely affected by systematic errors (like temperature dependence, ground calibration …).When careful attention is being payed to describe the 3D structure of the spacecraft/payload/board/chip, and with the use of proper ground calibrations, SEU counters from EDAC provide very good feedback to investigate on environment specification model margins.

In all cases, AP8 min is found to provide closer predictions to observations than AP9 V1.30.001 Mean or Perturbed mean-median out of 40 scenarios. While in the 660-1336 km altitude range, AP8 underestimates proton fluxes with energy greater than 30 MeV by 10-20% and AP9 V1.30.001 Mean or Perturbed mean-median out of 40 scenarios overestimates the observations by 40-110%. At the outer edge of the energetic proton belt, in the 8070 km altitude range, both AP8 min and AP9 1.30.001 Mean or Perturbed mean-median out of 40 scenarios overestimate in-situ observations respectively by 160% and 1240%. Note that in this latter case, validation has been performed using only one set of flight data (TID) and further investigations should be performed using cumulated SEUs from EDAC counter for example. It would allow to double check that the deviations obtained are not affected by possible systematic errors (temperature dependence, ground calibration …).

V. ACKNOWLEDGMENTS

The authors wish to thanks P. Calvel from Thales Alenia Space for providing the radiation 3D model for JASON-2 spacecraft, the FASTRAD sectoring analysis for the SIRAL payload and for O3B and the SEU counter measurements from CRYOSAT-2/SIRAL EDAC.

The authors wish to thanks also the CNES R&T program for their full support to this activity.

VII. REFERENCES

[1] D.M. Sawyer and J.I. Vette, "AP8 trapped proton model environment for solar maximum and minimum", *NSSDC/WDC-A-R&S 76-06*, Natl. Space Sci. Data Cent., Greenbelt, MD, 1976.

[2] E. J. Daly, J. Lemaire, D. Heynderickx and D.J. Rodgers, “Problems with Models of the Radiation Belts”, *IEEE Trans. Nucl. Sci*., vol. 43, no. 2, pp. 403-415, 1996.

[3] D.J. Rodgers, “Empirical Radiation Belt Models”, *AGU Geophysical Monograph 1997*, 1997.

[4] G.P. Ginet; , T. P. O’Brien, S. L. Huston, W. R. Johnston, T. B. Guild, R. Friedel, C. D. Lindstrom, C. J. Roth, P. Whelan, R. A. Quinn, D. Madden, S. Morley and Y.-J. Su, ”AE9, AP9 and SPM: new models for specifying the trapped energetic particle and space plasma environment”, *Space science reviews*, vol. 179, no. 1-4, pp. 579-615, 2013.

[5] Celestrak website: [Online]. Available: http://www.celestrak.com/NORAD/elements/

[6] Celestrak website [Online]. Available: http://celestrak.com/NORAD/documentation/spacetrk.pdf

[7] D. Boscher, A. Sicard-Piet, D. Lazaro, T. Cayton and G. Rolland, "A New Proton Model for Low Altitude High Energy Specification," in IEEE Transactions on Nuclear Science, vol. 61, no. 6, pp. 3401-3407, Dec. 2014. doi: 10.1109/TNS.2014.2365214.

[8] S. Bourdarie, C. Inguimbert, J.-R. Vaillé, P. Calvel, A. Sicard-Piet, D. Falguere, E. Lorfèvre, R. Ecoffet, C. Poivey, “Benchmarking ionizing space environment models”, RADECS 2016 proceedings.

[9] FASTRAD website: [Online]. Available: http://www.fastrad.net/

[10] F. Bezerra, R. Ecoffet, E. Lorfèvre, A. Samaras and C. Deneau, “CARMEN2/MEX: An in-flight laboratory for the observation of radiation effects on electronic devices”, 2011 12th European Conference on Radiation and Its Effects on Components and Systems, Sevilla, pp. 607-614; 2011.

[11] L. Dusseau, D. Plattard, J.-R. Vaillé, G. Polge, G. Ranchoux, F. Saigné, J. Fesquet, R. Ecoffet, and J. Gasiot, “An integrated sensor using optically stimulated luminescence for in flight dosimetry”, *IEEE Trans. Nucl*. Sci., vol. 47, no. 6, pp. 2412–2416, 2000.

[12] D. Plattard, G. Ranchoux, L. Dusseau, G. Polge, J.-R. Vaille, J. Gasiot, J. Fesquet, R. Ecoffet, and N. Iborra-Brassart, “Characterization of an integrated sensor using optically stimulate luminescence for in-flight dosimetry”, *IEEE Trans. Nucl. Sci*., vol. 49, no. 6, pp. 1322–1326, 2002.

[13] J.-R. Vaillé, F. Ravotti, P. Garcia, M. Glaser, S. Matias, K. Idri, J. Boch, E. Lorfèvre, P. J. McNulty, F. Saigné, and L. Dusseau, “Online dosimetry based on optically stimulated luminescence materials”, *IEEE Trans. Nucl. Sci*., vol. 52, no. 6, pp. 2578–2582, 2005.

[14] P. Garcia, J.-R. Vaillé, D. Benoit, F. Ravotti, L. Artola, B. Sagnes, E. Lorfèvre, F. Bezerra, and L. Dusseau, “Study of the thermal behavior of the OSL integrated sensor response”, I*EEE Trans. Nucl. Sci*., vol. 54, no. 6, pp. 2272–2275, 2007.

[15] C. Deneau, J.-R. Vaillé, L. Dusseau, J. Mekki, P. Garcia, F. Bezerra, E. Lorfèvre, and R. Ecoffet, "First In-Flight Data Analysis of Displacement Damage on the OSL Sensor On-Board CARMEN-2", *IEEE Trans. Nucl. Sci*., vol. 58, no.3, pp. 939–944, 2011.

[16] P. Garcia, J.-R. Vaillé, D. Benoit, H. Chabane, G. Berger, K. Idri, J. Boch, B. Sagnes, F. Saigné, E. Lorfèvre, F. Bezerra, and L. Dusseau, “Simultaneous evaluation of TID and displacement damage dose using a single OSL sensor”, *IEEE Trans. Nucl. Sci*., vol. 53, no. 6, pp. 3713–3717, 2006.

[17] D. Boscher, Cayton, T.; Maget, V.; Bourdarie, S.; Lazaro, D.; Baldran, T.; Bourdoux, P.; Lorfevre, E.; Rolland, G.; Ecoffet, R., "In-Flight Measurements of Radiation Environment on Board the Argentinean Satellite SAC-D," in IEEE Transactions on Nuclear Science, vol. 61, no. 6, pp. 3395-3400, Dec. 2014. doi: 10.1109/TNS.2014.2365212.

[18] C. Poivey, B. Doucin, M. Bruggemann and R. Harboe-Sorensen, "Radiation characterisation of commercially available 1 Mbit/4 Mbit SRAMs for space applications," Radiation Effects Data Workshop, 1998. IEEE, Newport Beach, CA, pp. 68-73, 1998.

[19] D. Novak, Granholm L., Kerek A., Milito G., Molnair J., Norlin L.O., Rathsman P., Szekely G., "In flight SEU tests on the European SMART-1 spacecraft," 2005 8th European Conference on Radiation and Its Effects on Components and Systems, Cap d'Agde, pp. PH1-1-PH1-3, 2005., doi: 10.1109/RADECS.2005.4365620.

[20] B. Vandevelde, “Proton test report: single event effects M65608E (DC1203) Rad. Tolerant 128k × 8, 5-Volt SRAM From ATMEL”, TRAD/TP/M65608/1203/ESA/BV/1312, 2013.

[21] L.S. Waters ed., MCNPx user’s manual Version 2.3.0, LA-UR-02-2607, April 2012.

[22] Denise B. Pelowitz editor, MCNPx user’s manual Version 2.7.0, LA-CP-11-00438, , April 2011.

[23] S. Bourdarie, Falguere, D.; Inguimbert, C.; Deneau, C.; Vaillé, J.-R.; Lorfèvre, E.; Ecoffet, R., "Correlation of in-flight displacement damage on the OSL sensor with space environment on-board Jason-2 spacecraft," in IEEE Transactions on Nuclear Science, vol. 61, no. 4, pp. 1643-1647, Aug. 2014., doi: 10.1109/TNS.2014.2315832.

[24] A. Jaksic, “New RADFETs for space applications,” in ESA-ESTEC, 2009